Influence of osteoporosis and mechanical loading on bone around osseointegrated dental implants: A rodent study

陳, 曦

journal of the mechanical behavior of biomedical materials 123 (2021) 104771

Contents lists available at ScienceDirect

Journal of the Mechanical Behavior of Biomedical Materials

journal homepage: www.elsevier.com/locate/jmbbm

Influence of osteoporosis and mechanical loading on bone around osseointegrated dental implants: A rodent study

Xi Chen, Yasuko Moriyama *, Yoko Takemura, Maho Rokuta, Yasunori Ayukawa

Section of Implant and Rehabilitative Dentistry, Division of Oral Rehabilitation, Faculty of Dental Science, Kyushu University, 3-1-1 Maidashi, Higashi-ku, Fukuoka, 812-8582, Japan

ARTICLE INFO

Keywords:
Osteoporosis
Peri-implant bone
Mechanical loading
Osteocyte

ABSTRACT

This study aimed to evaluate the influence of estrogen deficiency and mechanical loading on bone around osseointegrated dental implants in a rat jaw model. The maxillary right first molars of 36 rats were extracted. One week later, the rats were divided into an unloaded group and a loaded group; short head implants and long head implants were inserted respectively. Nine weeks after implantation, the rats were further subjected to ovariectomy (OVX) or sham surgery. All animals were euthanized 21 weeks after OVX. Micro-computed tomography, histological and histomorphometrical evaluation were undertaken. Systemic bone mineral density and bone volume fraction decreased in OVX groups compared with the sham controls. Histomorphometrical observation indicated that unloaded OVX group showed significantly damaged osseointegration and bone loss versus the loaded OVX group. Both the bone density (BD) inside the peri-implant grooves and the percentage of bone-to-implant contact (BIC) were lower in the OVX groups than in the sham-surgery groups, although mechanical loading increased the BIC and BD in the loaded OVX group compared with the unloaded OVX group. An increased number of positive cells for tartrate-resistant acid phosphatase was observed in the OVX groups versus the sham controls. The percentage of sclerostin-positive osteocytes was lower under loaded compared with unloaded conditions in both the OVX groups and the sham controls. In conclusion, estrogen deficiency could be a risk factor for the long-term stability of osseointegrated implants, while mechanical loading could attenuate the negative influence of estrogen deficiency on bone formation and osseointegration.

1. Introduction

Dental implants are widely used because of their ability to restore masticatory function and esthetics. Before implant surgery is undertaken, the patient's general health condition is usually thoroughly assessed. However, even if the patient's health is satisfactory at the time of implant placement, health conditions often worsen as the patient ages.

Osteoporosis is a systemic skeletal disease, and post-menopausal osteoporosis, which is characterized by a decrease in bone mass and bone quality, is mainly caused by an estrogen deficiency (Sozen et al., 2017; Ji and Yu, 2015). Because bone strength is considered important for dental implantology, the impact of osteoporosis on implant treatment has become a focus of attention, with many studies finding that osteoporosis can be a risk factor in the outcome of dental implants (Duarte et al., 2003; August et al., 2001; Alsaadi et al., 2007; Merheb et al., 2016; Li et al., 2017; Giro et al., 2011; Yamazaki et al., 1999). There are few long-term studies into the changes in peri-implant bone when a healthy implant is later affected by osteoporosis.

In the limited previous animal studies, the femur or tibia was often chosen as the location for dental implantation (Li et al., 2017; Giro et al., 2011). However, these conditions differ from the oral environment, not only because dental implants are constantly exposed to chemical and bacterial attacks, but also because mechanical loading, such as mastication, is a major factor that should be considered during the functional period of the implant. Additionally, the biomechanics of the jawbone differ from those of long bones (Bagi et al., 2011; Bidez and Misch, 1992; Van der Meulen et al., 2001), and the transfer and redistribution of stress inside the trabecular bone around implants under loading conditions are strongly influenced by the bone quality and structure (Delgado-Ruiz et al., 2019; Wirth et al., 2011; Ruffoni et al., 2012). Accordingly, it is important to use the jawbone to study the influence of mechanical loading on the bone surrounding the implant.

Therefore, in our experimental model, ovariectomies were

* Corresponding author.
E-mail address: kabay@dent.kyushu-u.ac.jp (Y. Moriyama).

https://doi.org/10.1016/j.jmbbm.2021.104771
Received 1 June 2021; Received in revised form 6 August 2021; Accepted 8 August 2021
Available online 10 August 2021

performed after implants were placed in the maxilla. The aim of the present study was to investigate the effect of postmenopausal osteoporosis after the acquisition of osseointegration on the bone response to mechanical loading and unloading using a rat oral implantation model.

2. Materials and methods

2.1. Animals

All animal procedures and activities were approved by the ethical committee for animal research of Kyushu University (approval number: A19-196-0, A21-270-0) and conform to the ARRIVE guidelines (Percie du Sert et al., 2020). In total, 36 female Wistar rats were used in this study. A required sample size of 9 was determined by performing a power analysis based on a previous study (Viera-Negron et al., 2008). These animals were housed under identical conditions and fed a standard commercial rodent chow containing 1.25% calcium, 1.06% phosphate, and 2.0 IU/g of vitamin D3 (CE-2; CLEA Japan, Inc., Tokyo, Japan). Water was available *ad libitum*.

2.2. Surgical procedures

Female Wistar rats (5 weeks old, weight 100–105 g, n = 9 each group) were used for the experiment. A study design schema is presented in Fig. 1(a). The maxillary right first molar was extracted under general anesthesia. One week after tooth extraction, implants were placed based on the method used in a previous study with slight modification (Takemura et al., 2019). Briefly, the bone cavities were drilled with a K-Reamer (#80–#120; Torpan, Maillefer, Switzerland) to prepare an implant socket. Machined surface, screw-shaped pure titanium implants (Sky Blue, Fukuoka, Japan) [Fig. 1(b)] were then screwed into the cavities. The rats were firstly divided into an unloaded group (n = 18) and a loaded group (n = 18). For rats in the unloaded group, implants with a short transmucosal section (type 1: 2 mm diameter, 3 mm in length, 0.5 mm transmucosal, 2.5 mm intrabony) were screwed into the cavities at a height of 0.5 mm below the marginal gingiva. For rats in the loaded group, implants with a long transmucosal section (type 2: 2 mm diameter, 4 mm in length, 1.5 mm transmucosal, 2.5 mm intrabony) were screwed into the cavities at a height determined by the height of the left first molar and the right second molar. All implants were checked once a week after placement to ensure that the implant was integrated with the bone without any movement, and that dental plaque

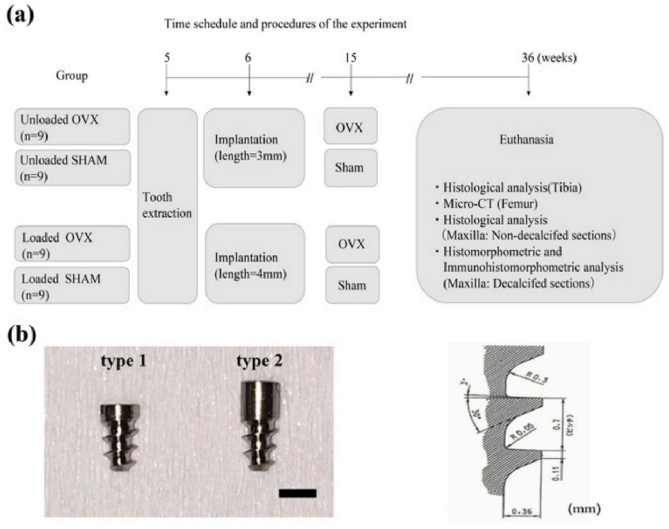

Fig. 1. (a) Study design: time schedule and procedures for the study. (b) Photographs and design of implants placed in the unloaded groups (type1) and the loaded groups (type 2) (bar = 2 mm).

was removed regularly.

Nine weeks after implantation, the rats were further divided into an OVX group and a SHAM group. Rats in the OVX groups received a bilateral ovariectomy using a dorsal approach method (Kharode et al., 2008) and rats in SHAM groups underwent the same procedure without removing the ovaries. At the age of 36 weeks, all animals were euthanized and perfused intracardially with heparinized saline solution, followed by 4% paraformaldehyde fixative (pH 7.4).

2.3. Histological preparation and histomorphometrical evaluation of the tibia

To verify the onset of osteoporosis after the ovariectomy, the left tibiae were harvested (n = 3 each group), immersed in 4% paraformaldehyde fixative for 48 h at 4 °C, decalcified in 20% ethylene diamine tetra-acetic acid (EDTA) solution (pH 7.4) for 4 weeks at 4 °C, and then paraffin-embedded after dehydration with a graded ethanol series and xylene. The samples were sectioned at 3-μm thickness (REM710, Yamato Kohki Industrial, Asaka, Japan) and stained with hematoxylin and eosin (H&E). All sections were observed and photographed with a light microscope (BIOREVO BZ-9000, Keyence, Osaka, Japan).

2.4. Micro-computed tomography (μ-CT) evaluation of the femur

The left femur was scanned by μ-CT (SkyScan 1076; Bruker microCT, Kontich, Belgium; tube current: 201 μA; voltage: 48 kV; pixel size: 9 μm). After reconstruction of the images by software (NRecon, Bruker), the bone mineral density (BMD) and bone volume fraction (bone volume/tissue volume: BV/TV) of four anatomical sites were evaluated according to the manufacturer's method note (Bruker, 2013). Specifically, trabecular region of the intertrochanteric crest area, the lesser trochanter area, the distal body area and the epicondyle area were measured using image analysis software (CTAn, Bruker). The three-dimensional ROI of intertrochanteric crest area was from the cross-section where the femoral neck and quadrate tubercle completely meet and extend for 50 slices distally. The three-dimensional ROI of the lesser trochanter area was from the maximum cross-section of the lesser trochanter and extend for 50 slices distally. The three-dimensional ROI of the distal body area was from the cross-section where the condyle completely disappeared and extend for 50 slices proximally. And the three-dimensional ROI of the epicondyle area was from the cross-section where the four quadrants of the femoral growth plate completely meet and extend for 50 slices proximally. The beginning cross-section of each measurement area shown in Fig. 2(b).

2.5. Histological preparation and histomorphometrical evaluation of the peri-implant bone

2.5.1. Non-decalcified sections

Maxillae (n = 1 each group) were fixed in 70% ethyl alcohol for 3 days immediately after harvesting. The blocks were stained as a whole in 1% basic fuchsin hydrochloride in a graded series of alcohols under vacuum according to a standard protocol (Burr and Hooser, 1995). After staining, the blocks were embedded using methlyl methacrylate. After polymerization, sections were cut using a saw microtome (Leica SP1600, Leica biosystems, Wetzlar, Germany), and were ground and polished to a thickness of 70 μm using a grinding system (Metaserv250, Buehler, IL, USA).

2.5.2. Decalcified sections

Maxillae (n = 8 each group) were immersed in 4% paraformaldehyde fixative for 48 h at 4 °C and decalcified in 20% EDTA (pH 7.4) for 3 weeks at 4 °C. The implants were carefully removed via inverse rotation. The maxillae were snap frozen in dry ice/isopentane and 10 μm buccopalatal sections were cut with a cryostat (CM 1860, Leica Biosystems,

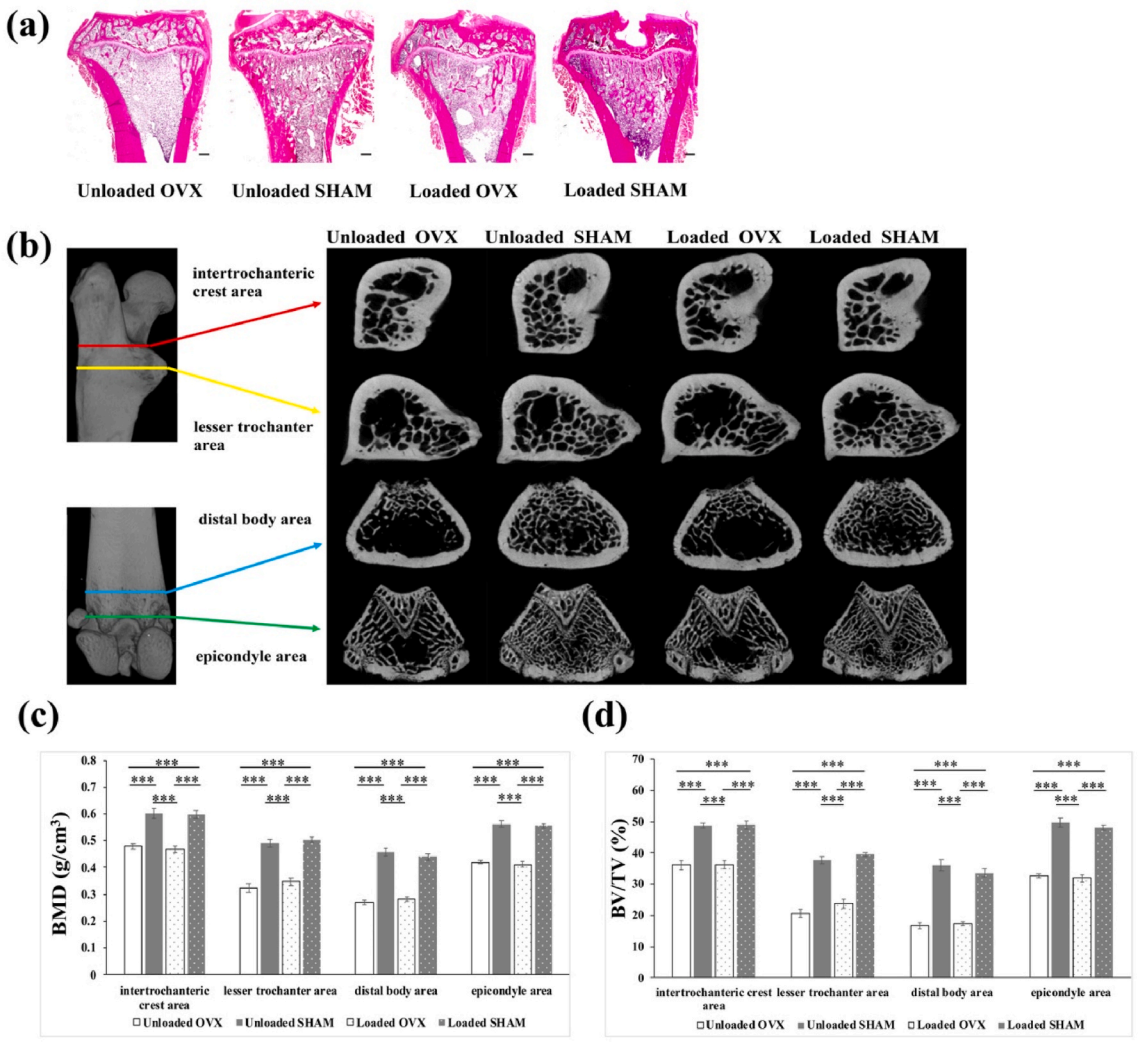

Fig. 2. (a) Tibia sections stained with hematoxylin and eosin (bar = 500 μm). (b) Radiographs of femur in each group: the first cross section of each area for morphometeic analysis was shown. (c) Bone mineral density (BMD) of four anatomical sites in each group. ANOVA with Bonferroni test (n = 9); ***p < 0.001 between the indicated groups. (d) Bone volume/tissue volume (BV/TV) of four anatomical sites in each group. ANOVA with Bonferroni test (n = 9); ***p < 0.001 between the indicated groups.

Wetzlar, Germany) at −20 °C after being immersed in 20% sucrose in 0.1 M phosphate buffer at 4 °C overnight and then embedded in O.C.T compound (Sakura Finetek, Tokyo, Japan). H&E staining was performed according to standard protocols. The bone-implant contact percentage (BIC) and bone density (BD) were measured based on the methods used in a previous study (Munhoz et al., 2011). The BIC was defined as the ratio of the length in contact with the bone surface to the total length of the implant from the lower border of the first thread to the upper border of the third buccal thread. BD was defined as the ratio of the total area of bone inside the second and the third buccal grooves to the total tissue area inside the second and third buccal grooves. Tartrate-resistant acid phosphatase (TRAP) staining was conducted using a stain kit according to standard instructions (Fujifilm Wako Pure Chemical, Osaka, Japan) to detect TRAP-positive cells and the number of osteoclasts inside the grooves was counted. Sclerostin was examined by immunohistochemical staining. Briefly, rabbit polyclonal anti-sclerostin antibody (1:50 dilution; Abcam, Cambridge, UK) was used as the primary antibody followed by biotinylated goat anti-rabbit IgG (1:200 dilution, Vector Laboratories, Burlingame, CA, USA) as the secondary antibody. After treated with peroxidase-conjugated avidin to produce an avidin−biotin complex (Vectastain, Vector Laboratories), the immunoreactivity was visualized using 3,3′-diaminobenzidine tetrahydrochloride (DAB) (Nacalai Tesque, Kyoto, Japan) and the sections were counterstained with hematoxylin. Sclerostin-positive osteocytes (brown staining) and total osteocytes inside the grooves were counted and the percentage of sclerostin-positive osteocytes to the total number of osteocytes inside the grooves was calculated.

All sections were observed and photographed with a light microscope (BIOREVO BZ-9000, Keyence). Images were analyzed by image software included in the microscope and ImageJ 1.53 (National Institute of Health, Bethesda, MD, USA).

2.6. Statistical analysis

After verifying normal distribution and homoscedasticity of the data with the Shapiro–Wilk test and Levene's test ($P > 0.05$), the femur data were compared by Bonferroni test, and all other data were analyzed with Student's t-test or Welch's *t*-test. Values of $p < 0.05$ were considered to be statistically significant. Data are indicated as the mean ± standard error of the mean (SEM). The statistical analysis was conducted with SPSS Statistics 19 software (IBM, Armonk, NY, USA).

3. Results

3.1. Verification of the postmenopausal osteoporosis-like rat model

3.1.1. Histological analysis of the tibia

An apparent decrease in trabecular density and loss of trabecular connectivity were observed in the OVX groups when compared with the SHAM groups [Fig. 2(a)].

3.1.2. Micro-computed tomography (μ-CT) of the femur

The BMD and BV/TV of the four anatomical sites of the femur (intertrochanteric crest area, lesser trochanter area, distal body area and epicondyle area) were measured [Fig. 2(b)]. Statistically significant differences were evident in both BMD and BV/TV, which indicates apparent bone loss in the OVX groups. There were no statistically significant differences between the unloaded OVX group and the loaded OVX group, nor between the unloaded SHAM group and the loaded SHAM group, which can be considered as evidence that the unloaded and loaded OVX groups, and the unloaded and loaded SHAM groups had similar levels of osteoporosis [Fig. 2(c and d)].

3.2. Evaluation of the bone around the implant

3.2.1. Histological analysis of non-decalcified sections

Implants not removed from the bone could be seen in the non-decalcified sections. Massive formation of fibrous tissue at the bone-implant interface and obvious loss of peri-implant bone were observed in the unloaded OVX group. In the unloaded SHAM group, partial fibrous tissue invasion at the bone-implant interface was observed. No apparent peri-implant bone loss was observed but certain area revealed little of fibrous tissue invasion were present at the bone-implant interface in the loaded OVX group. In the loaded SHAM group, bone contact to the implant surface was observed and no apparent bone loss was detected (Fig. 3).

3.2.2. Histomorphometric and immunohistomorphometric analysis of decalcified sections

3.2.2.1. Bone density (BD). Decreased BD was observed in the OVX groups when compared with the SHAM groups, and statistically significant differences were recorded under both unloaded condition and loaded conditions [Fig. 4 (a), (b-I, II)]. BD was higher in the loaded OVX group than in the unloaded OVX group, and in the loaded SHAM group than in the unloaded SHAM group [Fig. 4(a), (b-III, IV)].

3.2.2.2. Percentage of bone-to-implant contact (BIC). The BIC of the unloaded OVX group was lower than that of the unloaded SHAM group, and the same tendency was shown when the loaded OVX group was compared with the loaded SHAM group [Fig. 4(a), (b-I, II)]. The BIC was higher in the loaded OVX group than in the unloaded OVX group, and was also higher in the loaded SHAM group than in the unloaded SHAM group [Fig. 4(a), (b-III, IV)].

3.2.2.3. Tartrate-resistant acid phosphatase (TRAP) staining. In both the unloaded and loaded groups, the number of osteoclasts inside the grooves in the OVX groups was significantly higher than that in the SHAM groups [Fig. 5 (a), (b-I, II)]. In both OVX and SHAM groups, the number of osteoclasts inside the grooves in the unloaded groups was significantly higher than that in the loaded groups [Fig. 5 (a), (b-III, IV)].

3.2.2.4. Numbers of osteocytes and percentage of sclerostin-positive osteocytes. No statistically significant differences were observed in the number of osteocytes between unloaded OVX and SHAM groups, loaded OVX and SHAM groups, unloaded OVX and loaded OVX groups, or between unloaded SHAM and loaded SHAM groups [Fig. 6(a), (b-I, II, III, IV)].

No statistically significant differences were observed in the percentage of sclerostin-positive osteocytes between unloaded OVX and SHAM groups, or between loaded OVX and SHAM groups [Fig. 6(a), (b-I, II)]. Conversely, the percentage of sclerostin-positive osteocytes under loaded conditions in the OVX and SHAM groups was significantly smaller than that of each unloaded group [Fig. 6 (a), (b-III, IV)].

4. Discussion

Ovariectomy in rats is acknowledged as the gold standard for inducing osteoporosis, and ovariectomized rats are widely used as a model for postmenopausal osteoporosis in humans (Wronski et al., 1989; Kalu, 1991; Johnston and Ward, 2015). To ensure that bone loss is caused by ovarian hormone deficiency, the ovariectomy should be performed after sexual maturation has occurred. A mature rat model shares many characteristics with early postmenopausal bone loss, and rats that receive ovariectomies at 3–6 months of age are widely used in research into alveolar bone loss (Johnston and Ward, 2015). Additionally, it has been proven that osseointegration around implants can be obtained at 1 month post-implantation in a rat maxilla model (Futami et al., 2000; Fujii et al., 1998). Taking these findings into consideration, after osseointegration had been achieved and the rats were sexual mature, bilateral ovariectomies were performed on 15-week-old rats to induce postmenopausal osteoporosis in the present study. The timing of the sacrifice of the rats was decided in reference to the results of estrogen-deficiency-associated bone loss studies in the maxilla which demonstrated that at least 3 months of observation is needed after ovariectomy to detect any obvious change in the bone structure (Du et al., 2015).

After the rats were sacrificed, we verified the level of systemic osteoporosis. H&E-stained tibiae showed that the trabecular structure was shorter and thinner in the OVX groups. Differences were apparent in the trabecular density and structure between the OVX groups and SHAM groups. Furthermore, BMD and BV/TV measurement using micro-CT revealed that the OVX groups showed apparent bone loss compared with the SHAM groups, although there were no statistically significant differences between the unloaded OVX group and the loaded OVX group, nor between the unloaded SHAM group and the loaded SHAM group. These results confirmed the successful modeling of rat

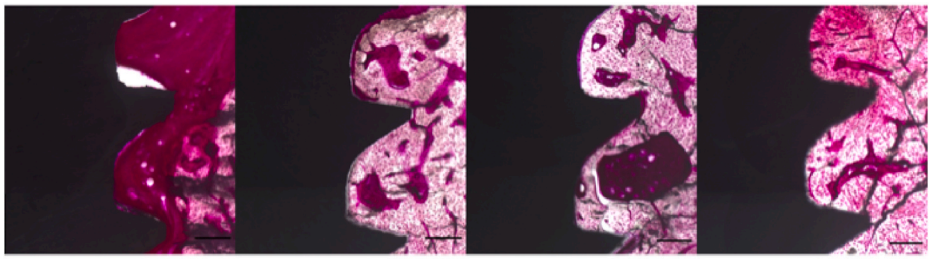

Fig. 3. Non-demineralized basic fuchsin stained sections of the implants (bar = 100 μm).

(a)

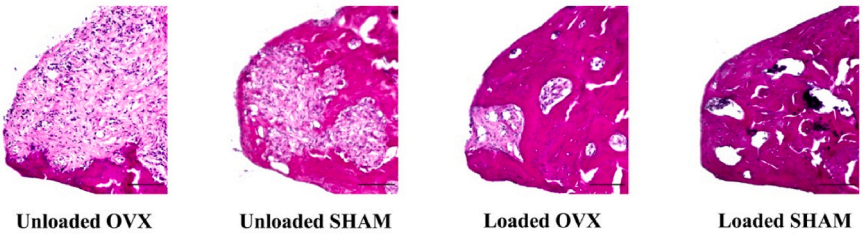

(b)

I

Parameters	Unloaded OVX	Unloaded SHAM	P value
BD (%)	27.04 ± 6.44	59.46 ± 5.53	0.002
BIC (%)	33.04 ± 11.35	74.07 ± 7.42	0.009

II

Parameters	Loaded OVX	Loaded SHAM	P value
BD (%)	60.82 ± 5.38	78.16 ± 4.84	0.031
BIC (%)	70.50 ± 7.86	92.33 ± 2.72	0.029 [w]

III

Parameters	Unloaded OVX	Loaded OVX	P value
BD (%)	27.04 ± 6.44	60.82 ± 5.38	0.001
BIC (%)	33.04 ± 11.35	70.50 ± 7.86	0.017

IV

Parameters	Unloaded SHAM	Loaded SHAM	P value
BD (%)	59.46 ± 5.53	78.16 ± 4.84	0.023
BIC (%)	74.07 ± 7.42	92.33 ± 2.72	0.047 [w]

Fig. 4. (a) Decalcified sections stained with hematoxylin and eosin (bar = 100 μm). (b) Result of bone density (BD) and bone-to-implant contact (BIC) in each group. Student's t-test (n = 8 each group, 3 sections per rat); [w]: Welch's *t*-test (n = 8 each group, 3 sections per rat).

(a)

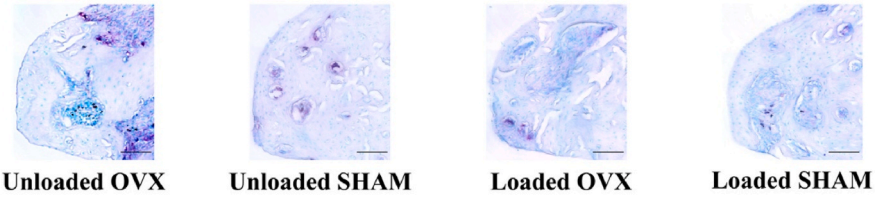

(b) I

Parameter	Unloaded OVX	Unloaded SHAM	P value
Number of osteoclasts (#/mm²)	57.89 ± 1.94	44.85 ± 3.82	0.009

II

Parameter	Loaded OVX	Loaded SHAM	P value
Number of osteoclasts (#/mm²)	40.61 ± 5.03	19.97 ± 4.87	0.011

III

Parameter	Unloaded OVX	Loaded OVX	P value
Number of osteoclasts (#/mm²)	57.89 ± 1.94	40.61 ± 5.03	0.011 [w]

IV

Parameter	Unloaded SHAM	Loaded SHAM	P value
Number of osteoclasts (#/mm²)	44.85 ± 3.82	19.97 ± 4.87	0.001

Fig. 5. (a) Tartrate-resistant acid phosphatase (TRAP) staining. Osteoclasts are stained red (bar = 100 μm). (b) The number of osteoclasts observed inside implant grooves. Student's t-test (n = 8 each group, 3 sections per rat); [w]: Welch's *t*-test (n = 8 each group, 3 sections per rat).

(a)

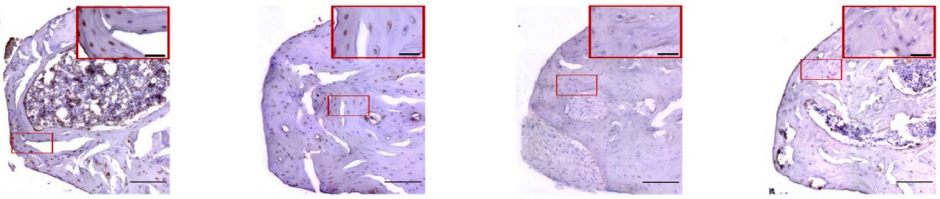

(b) I

Parameters	Unloaded OVX	Unloaded SHAM	P value
Number of osteocytes (#/mm²)	1478.35 ± 197.67	1749.93 ± 128.98	0.269
Percentage of sclerostin-positive osteocytes (%)	13.11 ± 2.25	11.61 ± 1.38	0.577

II

Parameters	Loaded OVX	Loaded SHAM	P value
Number of osteocytes (#/mm²)	1352.45 ± 119.04	1518.77 ± 108.67	0.320
Percentage of sclerostin-positive osteocytes (%)	5.08 ± 1.32	3.63 ± 0.72	0.350

III

Parameters	Unloaded OVX	Loaded OVX	P value
Number of osteocytes (#/mm²)	1478.35 ± 197.67	1352.45 ± 119.04	0.594
Percentage of sclerostin-positive osteocytes (%)	13.11 ± 2.25	5.08 ± 1.32	0.008

IV

Parameters	Unloaded SHAM	Loaded SHAM	P value
Number of osteocytes (#/mm²)	1749.93 ± 128.98	1518.77 ± 108.67	0.192
Percentage of sclerostin-positive osteocytes (%)	11.61 ± 1.38	3.63 ± 0.72	0.0001

Fig. 6. (a) Immunohistochemical staining for sclerostin: area in the little red window is digitally magnified into the big red window at the top right corner of each image. Sclerostin-positive osteocytes are stained brown and sclerostin-negative osteocytes are purple. (bar represents 100 μm for the image and 25 μm for the image in the big red window). (b) Numbers of osteocytes and percentage of sclerostin-positive osteocytes inside the implant grooves. Student's t-test (n = 8 each group, 3 sections per rat).

postmenopausal osteoporosis, allowing us to shift our focus to the comparison of peri-implant bone in the maxilla.

In conditions of estrogen deficiency, the lifespan of both osteoblasts and osteocytes is shortened and their function is impaired (Manolagas, 2000; Kousteni et al., 2001). Conversely, the lifespan of osteoclasts is prolonged (Kameda et al., 1997; Hughes et al., 1996) and their differentiation and resorption activity is increased (Kameda et al., 1997; Allison and McNamara, 2019). An imbalance in bone remodeling, in

which bone formation cannot keep up with resorption, results in significant trabecular bone loss (Dobbs et al., 1999). The decrease in BD around the implants and the increased number of osteoclasts in the OVX groups showed that the estrogen deficiency also influenced the bone around the implants placed before the onset of osteoporosis.

Osteocytes, the most abundant cells in the bone matrix, are highly mechanosensitive, and therefore play an important role (Klein-Nulend et al., 2012). They are sensitive to loading and can also regulate bone resorption in response to mechanical unloading and estrogen deficiency (Atkins and Findlay, 2012; Bellido, 2014). Sclerostin, which gained attention because of its strong association with bone formation and bone mass, is a glycoprotein made almost exclusively by osteocyte in bone and can inhibit osteoblast function (Atkins and Findlay, 2012; Winkler et al., 2003; Li et al., 2008). A higher percentage of sclerostin-positive cells and increased osteoclast numbers were found inside grooves under unloaded conditions, indicating that the bone loss was caused by superiority of bone resorption. Conversely, the percentage of sclerostin-positive cells decreased in the loaded SHAM and loaded OVX groups, indicating that the suppression of osteoblast function was weakened, allowing bone formation to contribute to an increase in BD. Although a decrease in both the percentage of sclerostin-positive cells and the number of osteoclasts was observed in the loaded OVX group, there were still statistically significant differences in BD when compared with the loaded SHAM group. It is considered that bone resorption is still enhanced in the loaded OVX group as evidenced by the statistically significant difference in osteoclast numbers compared with the loaded SHAM group, and that loading might contribute to reducing the gap between bone formation and resorption, however, a continuous imbalance of bone remodeling around the implant still seems to occur under OVX condition.

Under unloaded conditions, BD was lower in the OVX group than in the SHAM group, possibly as a result of the double effects of disuse and estrogen deficiency. Furthermore, both the non-decalcified sections and the BD and BIC results showed the same tendency towards not only significant bone loss around implants, but also an obvious decrease in contact between the implant surface and the bone around the implant in the unloaded OVX group when compared with the loaded OVX group. These findings indicate that mechanical loading contributes to the long-term stability of implants, given that it has been demonstrated that proper maintenance of osseointegration and bone mass around implants is important for a successful implant outcome (Merheb et al., 2016; Albrektsson et al., 2017).

Limitations associated with this study warrant mention. In the present study, we divided rats into unloaded and loaded groups by using implants with different lengths of head height and the results showed that mechanical loading contributed to an increase in the bone mass of peri-implant bone. It is commonly known that bone mass may decrease in the absence of mechanical stimuli, but the increase in bone mass is not always in proportion to the increase in the mechanical force, animal studies have shown that high loads lead to the formation of fibrous tissue at the bone-implant interface instead of direct bone contact with the implant surface. This is considered to be a major reason for poor outcomes in terms of implant survival (Isidor, 2006; Esaki et al., 2012) and some clinical evidences suggests that excessive loading is a cause of dental implant failure (Esposito et al., 2000; Mattheos et al., 2013). On this basis, it was considered that a high load is a risk factor for peri-implant bone loss after successful bone-to-implant osseointegration (Kim et al., 2005; Duyck et al., 2001; Isidor, 1996). On the other hand, estrogen plays an important role in regulating the mechanoresponsiveness of bone cells (Allison and McNamara, 2019; Joldersma et al., 2001), and it has been demonstrated that the ability of bone to respond to loading is reduced because the viability of osteocyte networks is compromised under conditions of estrogen deficiency (Tomkinson et al., 1998).

Consequently, in future studies it is essential to determine the range of loading forces that can promote an increase in bone mass. Because of the difficulty of placing implant that mimic those used in humans and simulates the similar occlusion pattern to human in small animals, so, further studies using large animals are required.

5. Conclusion

Estrogen deficiency has a deleterious effect on the long-term stability of osseointegrated dental implants. Although the results were still inferior to the bone around implants under normal systemic conditions, mechanical loading attenuated to some degree the negative influence of estrogen deficiency by increasing the bone mass and subsequently improving osseointegration in a postmenopausal osteoporosis-like rat model.

Credit authorship contribution statement

Xi Chen: Conceptualization, Methodology, Formal analysis, Investigation, Validation, Data curation, Writing—original draft preparation.

Yasuko Moriyama: Conceptualization, Methodology, Formal analysis, Validation, Data curation, Writing—review and editing.

Yoko Takemura: Formal analysis, Investigation, Validation.

Maho Rokuta: Investigation.

Yasunori Ayukawa: Conceptualization, Methodology, Validation, Writing—review and editing, Supervision.

Funding

This study was supported in part by JSPS KAKENHI Grant Number JP17K11757, JP20K10074 from Japan Society for the Promotion of Science.

Declaration of competing interest

The authors declare that they have no known competing financial interests or personal relationships that could have appeared to influence the work reported in this paper.

Acknowledgments

We thank Edanz Group (www.edanzediting.com/ac) for editing a draft of this manuscript.

References

Albrektsson, T., Chrcanovic, B., Östman, P.O., Sennerby, L., 2017. Initial and long-term crestal bone responses to modern dental implants. Periodontol 73, 41–50. https://doi.org/10.1111/prd.12176, 2000.

Allison, H., McNamara, L.M., 2019. Inhibition of osteoclastogenesis by mechanically stimulated osteoblasts is attenuated during estrogen deficiency. Am. J. Physiol. Cell Physiol. 317, C969–C982. https://doi.org/10.1152/ajpcell.00168.2019.

Alsaadi, G., Quirynen, M., Komárek, A., Van Steenberghe, D., 2007. Impact of local and systemic factors on the incidence of oral implant failures, up to abutment connection. J. Clin. Periodontol. 34, 610–617. https://doi.org/10.1111/j.1600-051X.2007.01077.x.

Atkins, G.J., Findlay, D.M., 2012. Osteocyte regulation of bone mineral: a little give and take. Osteoporos. Int. 23, 2067–2079. https://doi.org/10.1007/s00198-012-1915-z.

August, M., Chung, K., Chang, Y., Glowacki, J., 2001. Influence of estrogen status on endosseous implant osseointegration. J. Oral Maxillofac. Surg. 59, 1285–1289. https://doi.org/10.1053/joms.2001.27515.

Bagi, C.M., Berryman, E., Moalli, M.R., 2011. Comparative bone anatomy of commonly used laboratory animals: implications for drug discovery. Comp. Med. 61, 76–85.

Bellido, T., 2014. Osteocyte-driven bone remodeling. Calcif. Tissue Int. 94, 25–34. https://doi.org/10.1007/s00223-013-9774-y.

Bidez, M.W., Misch, C.E., 1992. Issue in bone mechanics related to oral implants. Implant Dent. 1, 289–294. https://doi.org/10.1097/00008505-199200140-00011.

Bruker, 2013. Bone Mineral Density (BMD) and Tissue Mineral Density (TMD) Calibration and Measurement Using Bruker microCT BMD Phantoms and CT-Analyser Software. Bruker, Kontich, Belgium.

Burr, D.B., Hooser, M., 1995. Alterations to the en bloc basic fuchsin staining protocol for the demonstration of microdamage produced in vivo. Bone 17, 431–433. https://doi.org/10.1016/S8756-3282(95)00241-3.

Delgado-Ruiz, R.A., Calvo-Guirado, J.L., Romanos, G.E., 2019. Effects of occlusal forces on the peri-implant-bone interface stability. Periodontol 81, 179–193. https://doi.org/10.1111/prd.12291, 2000.
Dobbs, M.B., Buckwalter, J., Saltzman, C., 1999. Osteoporosis: the increasing role of the orthopaedist. Iowa Orthop. J. 19, 43–52.
Du, Z., Steck, R., Doan, N., Woodruff, M.A., Ivanovski, S., Xiao, Y., 2015. Estrogen deficiency-associated bone loss in the maxilla: a methodology to quantify the changes in the maxillary intra-radicular alveolar bone in an ovariectomized rat osteoporosis model. Tissue Eng. C Methods 21, 458–466. https://doi.org/10.1089/ten.tec.2014.0268.
Duarte, P.M., Cesar Neto, J.B., Gonçalves, P.F., Sallum, E.A., Nociti, F.H., 2003. Estrogen deficiency affects bone healing around titanium implants: a histometric study in rats. Implant Dent. 12, 340–346. https://doi.org/10.1097/01.ID.0000099750.26582.4b.
Duyck, J., Rønold, H.J., Van Oosterwyck, H., Naert, I., Vander Sloten, J., Ellingsen, J.E., 2001. The influence of static and dynamic loading on marginal bone reactions around osseointegrated implants: an animal experimental study. Clin. Oral Implants Res. 12, 207–218. https://doi.org/10.1034/j.1600-0501.2001.012003207.x.
Esaki, D., Matsushita, Y., Ayukawa, Y., Sakai, N., Sawae, Y., Koyano, K., 2012. Relationship between magnitude of immediate loading and peri-implant osteogenesis in dogs. Clin. Oral Implants Res. 23, 1290–1296. https://doi.org/10.1111/j.1600-0501.2011.02305.x.
Esposito, M., Thomsen, P., Ericson, L.E., Sennerby, L., Lekholm, U., 2000. Histopathologic observations on late oral implant failures. Clin. Implant Dent. Relat. Res. 2, 18–32. https://doi.org/10.1111/j.1708-8208.2000.tb00103.x.
Fujii, N., Kusakari, H., Maeda, T., 1998. A histological study on tissue responses to titanium implantation in rat maxilla: the process of epithelial regeneration and bone reaction. J. Periodontol. 69, 485–495. https://doi.org/10.1902/jop.1998.69.4.485.
Futami, T., Fujii, N., Ohnishi, H., Taguchi, N., Kusakari, H., Ohshima, H., Maeda, T., 2000. Tissue response to titanium implants in the rat maxilla: ultrastructural and histochemical observations of the bone-titanium interface. J. Periodontol. 71, 287–298. https://doi.org/10.1902/jop.2000.71.2.287.
Giro, G., Coelho, P.G., Pereira, R.M.R., Jorgetti, V., Marcantonio, E., Orrico, S.R.P., 2011. The effect of oestrogen and alendronate therapies on postmenopausal bone loss around osseointegrated titanium implants. Clin. Oral Implants Res. 22, 259–264. https://doi.org/10.1111/j.1600-0501.2010.01989.x.
Hughes, D.E., Dai, A., Tiffee, J.C., Li, H.H., Mundy, G.R., Boyce, B.F., 1996. Estrogen promotes apoptosis of murine osteoclasts mediated byTGF-P. Nat. Med. 2, 1132–1136. https://doi.org/10.1038/nm1096-1132.
Isidor, F., 1996. Loss of osseointegration caused by occlusal load of oral implants: a clinical and radiographic study in monkeys. Clin. Oral Implants Res. 7, 143–152. https://doi.org/10.1034/j.1600-0501.1996.070208.x.
Isidor, F., 2006. Influence of forces on peri-implant bone. Clin. Oral Implants Res. 2, 8–18. https://doi.org/10.1111/j.1600-0501.2006.01360.x.
Ji, M.X., Yu, Q., 2015. Primary osteoporosis in postmenopausal women. Chronic Dis. Transl. Med. 1, 9–13. https://doi.org/10.1016/j.cdtm.2015.02.006.
Johnston, B.D., Ward, W.E., 2015. The ovariectomized rat as a model for studying alveolar bone loss in postmenopausal women. BioMed Res. Int. https://doi.org/10.1155/2015/635023.
Joldersma, M., Klein-Nulend, J., Oleksik, A.M., Heyligers, I.C., Burger, E.H., 2001. Estrogen enhances mechanical stress-induced prostaglandin production by bone cells from elderly women. Am. J. Physiol. Endocrinol. Metab. 280, 436–442. https://doi.org/10.1152/ajpendo.2001.280.3.e436.
Kalu, D.N., 1991. The ovariectomized rat model of postmenopausal bone loss. Bone Miner. 15, 175–191. https://doi.org/10.1016/0169-6009(91)90124-I.
Kameda, T., Mano, H., Yuasa, T., Mori, Y., Miyazawa, K., Shiokawa, M., Nakamaru, Y., Hiroi, E., Hiura, K., Kameda, A., Yang, N.N., Hakeda, Y., Kumegawa, M., 1997. Estrogen inhibits bone resorption by directly inducing apoptosis of the bone-resorbing osteoclasts. J. Exp. Med. 186, 489–495. https://doi.org/10.1084/jem.186.4.489.
Kharode, Y.P., Sharp, M.C., Bodine, P.V.N., 2008. Utility of the ovariectomized rat as a model for human osteoporosis in drug discovery. Methods Mol. Biol. 455, 111–124. https://doi.org/10.1007/978-1-59745-104-8_8.
Kim, Y., Oh, T.J., Misch, C.E., Wang, H.L., 2005. Occlusal considerations in implant therapy: clinical guidelines with biomechanical rationale. Clin. Oral Implants Res. 16, 26–35. https://doi.org/10.1111/j.1600-0501.2004.01067.x.
Klein-Nulend, J., Bacabac, R.G., Bakker, A.D., 2012. Mechanical loading and how it affects bone cells: the role of the osteocyte cytoskeleton in maintaining our skeleton. Eur. Cell. Mater. 24, 278–291. https://doi.org/10.22203/eCM.v024a20.
Kousteni, S., Bellido, T., Plotkin, L.I., O'Brien, C.A., Bodenner, D.L., Han, L., Han, K., DiGregorio, G.B., Katzenellenbogen, J.A., Katzenellenbogen, B.S., Roberson, P.K., Weinstein, R.S., Jilka, R.L., Manolagas, S.C., 2001. Nongenotropic, sex-nonspecific signaling through the estrogen or androgen receptors: dissociation from transcriptional activity. Cell 104, 719–730. https://doi.org/10.1016/s0092-8674(01)00268-9.
Li, X., Ominsky, M.S., Niu, Q.T., Sun, N., Daugherty, B., D'Agostin, D., Kurahara, C., Gao, Y., Cao, J., Gong, J., Asuncion, F., Barrero, M., Warmington, K., Dwyer, D., Stolina, M., Morony, S., Sarosi, I., Kostenuik, P.J., Lacey, D.L., Simonet, W.S., Ke, H. Z., Paszty, C., 2008. Targeted deletion of the sclerostin gene in mice results in increased bone formation and bone strength. J. Bone Miner. Res. 23, 860–869. https://doi.org/10.1359/jbmr.080216.
Li, Y., He, S., Hua, Y., Hu, J., 2017. Effect of osteoporosis on fixation of osseointegrated implants in rats. J. Biomed. Mater. Res. B Appl. Biomater. 105, 2426–2432. https://doi.org/10.1002/jbm.b.33787.
Manolagas, S.C., 2000. Birth and death of bone cells: basic regulatory mechanisms and implications for the pathogenesis and treatment of osteoporosis. Endocr. Rev. 21, 115–137. https://doi.org/10.1210/edrv.21.2.0395.
Mattheos, N., Schittek Janda, M., Zampelis, A., Chronopoulos, V., 2013. Reversible, Non-plaque-induced loss of osseointegration of successfully loaded dental implants. Clin. Oral Implants Res. 24, 347–354. https://doi.org/10.1111/clr.12009.
Merheb, J., Temmerman, A., Rasmusson, L., Kübler, A., Thor, A., Quirynen, M., 2016. Influence of skeletal and local bone density on dental implant stability in patients with osteoporosis. Clin. Implant Dent. Relat. Res. 18, 253–260. https://doi.org/10.1111/cid.12290.
Munhoz, E.A., Bodanezi, A., Cestari, T.M., Taga, R., Ferreira Junior, O., de Carvalho, P.S. P., 2011. Biomechanical and microscopic response of bone to titanium implants in the presence of inorganic grafts. J. Oral Implantol. 37, 19–25. https://doi.org/10.1563/AAID-JOI-D-09-00086.
Percie du Sert, N., Hurst, V., Ahluwalia, A., Alam, S., Avey, M.T., Baker, M., Browne, W. J., Clark, A., Cuthill, I.C., Dirnagl, U., Emerson, M., Garner, P., Holgate, S.T., Howells, D.W., Karp, N.A., Lazic, S.E., Lidster, K., MacCallum, C.J., Macleod, M., Pearl, E.J., Petersen, O.H., Rawle, F., Reynolds, P., Rooney, K., Sena, E.S., Silberberg, S.D., Steckler, T., Würbel, H., 2020. The arrive guidelines 2.0: updated guidelines for reporting animal research. PLoS Biol. 18, e3000410 https://doi.org/10.1371/journal.pbio.3000410.
Ruffoni, D., Müller, R., Van Lenthe, G.H., 2012. Mechanisms of reduced implant stability in osteoporotic bone. Biomech. Model. Mechanobiol. 11, 313–323. https://doi.org/10.1007/s10237-011-0312-4.
Sozen, T., Ozisik, L., Basaran, N.C., 2017. An overview and management of osteoporosis. Eur. J. Rheumatol. 4, 46–56. https://doi.org/10.5152/eurjrheum.2016.048.
Takemura, Y., Moriyama, Y., Ayukawa, Y., Kurata, K., Rakhmatia, Y.D., Koyano, K., 2019. Mechanical loading induced osteocyte apoptosis and connexin 43 expression in three-dimensional cell culture and dental implant model. J. Biomed. Mater. Res. 107, 815–827. https://doi.org/10.1002/jbm.a.36597.
Tomkinson, A., Gevers, E.F., Wit, J.M., Reeve, J., Noble, B.S., 1998. The role of estrogen in the control of rat osteocyte apoptosis. J. Bone Miner. Res. 13, 1243–1250. https://doi.org/10.1359/jbmr.1998.13.8.1243.
Van der Meulen, M.C., Jepsen, K.J., Mikić, B., 2001. Understanding bone strength: size isn't everything. Bone 29, 101–104. https://doi.org/10.1016/S8756-3282(01)00491-4.
Viera-Negron, Y.E., Ruan, W., Winger, J.N., Hou, X., Sharawy, M.M., Borke, J.L., 2008. Effect of ovariectomy and alendronate on implant osseointegration in rat maxillary bone. J. Oral Implantol. 34, 76–82. https://doi.org/10.1563/1548-1336(2008)34[76:EOOAAO]2.0.CO;2.
Winkler, D.G., Sutherland, M.K., Geoghegan, J.C., Yu, C., Hayes, T., Skonier, J.E., Shpektor, D., Jonas, M., Kovacevich, B.R., Staehling-Hampton, K., Appleby, M., Brunkow, M.E., Latham, J.A., 2003. Osteocyte control of bone formation via sclerostin, a novel BMP antagonist. EMBO J. 22, 6267–6276. https://doi.org/10.1093/emboj/cdg599.
Wirth, A.J., Goldhahn, J., Flaig, C., Arbenz, P., Müller, R., Van Lenthe, G.H., 2011. Implant stability is affected by local bone microstructural quality. Bone 49, 473–478. https://doi.org/10.1016/j.bone.2011.05.001.
Wronski, T.J., Dann, L.M., Scott, K.S., Cintrón, M., 1989. Long-term effects of ovariectomy and aging on the rat skeleton. Calcif. Tissue Int. 45, 360–366. https://doi.org/10.1007/BF02556007.
Yamazaki, M., Shirota, T., Tokugawa, Y., Motohashi, M., Ohno, K., Michi, K., Yamaguchi, A., 1999. Bone reactions to titanium screw implants in ovariectomized animals. Oral Surg. Oral Med. Oral Pathol. Oral Radiol. Endod. 87, 411–418. https://doi.org/10.1016/S1079-2104(99)70239-8.